Transaction E: Industrial Engineering
Vol. 16, No. 2, pp. 114–127

SCIENTIA IRANICA

Fuzzy Image Processing for Diagnosing Inflammation in Pulmonary Biopsies

M.H. Fazel Zarandi[1,*], M. Moeen[2], Sh. Norouzzadeh[1] and Sh. Teimourian[2]

Abstract. *This paper proposes a new approach to diagnose the degree of inflammation in digital images of pulmonary biopsies, provided by a digital camera through a microscope. Diagnosing is done by detecting thick epithelium cell layers around the vessels and bronchus in tissue images. For analyzing the complex images of tissue, a fuzzy image processing procedure consisting of five main stages is presented. The first stage is decreasing the complexity of the images by using image pre-processing methods for enhancement and smoothing the image with a Gaussian low pass filter in order to highlight important details and ignore the unnecessary parts of the image. The second stage is segmentation by using a fuzzy c-means clustering algorithm and fuzzy canny edge detection. This step works as a data reduction method as well as object recognition. Feature extraction, the third stage, will be done by using a fuzzy Hough transform. After extracting features such as bronchioles and vessels from the image, the fourth stage will be analysis and reasoning by a fuzzy inference system, which is a hybrid of the Mamdani and Logical modeling system with a Yager parametric operator. The last stage is tuning system parameters and the learning process with a feed forward neural network. The output of the proposed algorithm is the degree of inflammation inferred by the fuzzy inference system. The proposed approach is user friendly with low computational time and the results are more precise, reliable and acceptable to experts and physicians.*

Keywords: *Image processing; Fuzzy modeling; Fuzzy cluster analysis; Inflammation; Pulmonary; Canny edge detection; Hough transform; RGB image.*

INTRODUCTION

As technology has thrived during the past years, air pollution has increased and become the cause of many respiratory diseases. Diagnosis of these primary problems can prevent many diseases and catastrophes such as asthma and lung cancer. However, as preliminary diseases become more prevalent, we need to improve current diagnostic techniques to provide patients with better treatment options. In this study, we are going to develop a model to diagnose allergic asthma, which replicates the chronic inflammatory and epithelial changes of the vessels and bronchioles in pulmonary biopsies. To study the mechanisms of the remodeling processes and the relationship between resulting structural changes and airway dysfunction, it is crucial that the methods used to quantify these structural changes are well characterized, reproducible and responsive [1]. A morphometric technique is characterized to quantify changes in the extra cellular matrix and contractile tissue as two indices of airway remolding [2]. Accumulation of inflammatory cells and exudates increases the airway smooth muscle mass [3]. The deposition of connective tissue and epithelial hyperplasic may all contribute to thickening of the airway wall, which appears to be the basis for excessive diminution of the airflow that accompanies broncho-constriction in asthmatics [4]. The type of coloring for the used biopsies is Hematoxylin Cromotrop $2-r$ which is used widely for pulmonary biopsies.

Accurate detection of the vessel/bronchiole boundaries in images is crucial to the diagnosis of inflammation. However, the tissue images are very

1. *Department of Industrial Engineering, Amirkabir University of Technology, Tehran, P.O. Box 15875-4413, Iran.*
2. *Immunology, Asthma and Allergy Research Institute, Tehran University of Medical Sciences, Tehran, P.O. Box 14185-863, Iran.*
*. *Corresponding author. E-mail: zarandi@aut.ac.ir*

Received 24 October 2007; received in revised form 10 December 2008; accepted 25 May 2009

complicated and the boundaries between the objects are fuzzy. Moreover, weak edges make the images inherently difficult to segment. Furthermore, the quality of an image depends on the type and direction of the digital camera for imaging. All these factors make the analysis too challenging.

The focus of this research is to design, implement and evaluate automated algorithms to diagnose the degree of inflammation in digital images of pulmonary biopsies through the current and proposed image processing algorithms, based on fuzzy logic. A sample of a pulmonary tissue image is demonstrated in Figure 1. For analyzing this complex image of tissue, a fuzzy image processing procedure consisting of five main stages is presented. The first stage is decreasing the complexity of the images by using image preprocessing methods for enhancement and smoothing the image with a Gaussian low pass filter. The second stage is segmentation using a fuzzy c-means clustering algorithm and fuzzy canny edge detection. Feature extraction, the third stage, will be done by using the fuzzy Hough transform. After extracting features such as bronchioles and vessels from the image, the fourth stage will be analysis and reasoning by a fuzzy inference system, which is a hybrid of the Mamdani and Logical modeling system with a Yager parametric operator. The last stage is tuning the system parameters and the learning process with a feed forward neural network. The output of the proposed algorithm is the degree of inflammation inferred by the fuzzy inference system.

The rest of this paper is organized as follows: In the following section, the existing literature on medical fuzzy image processing is briefly reviewed. Then, the proposed approach is introduced and its main components and details are described. Following that, the method of learning and tuning of parameters of the proposed method is presented. Later, the performance of the method via experimental results and some quantitative measures are validated. Finally, the conclusion and future works are discussed.

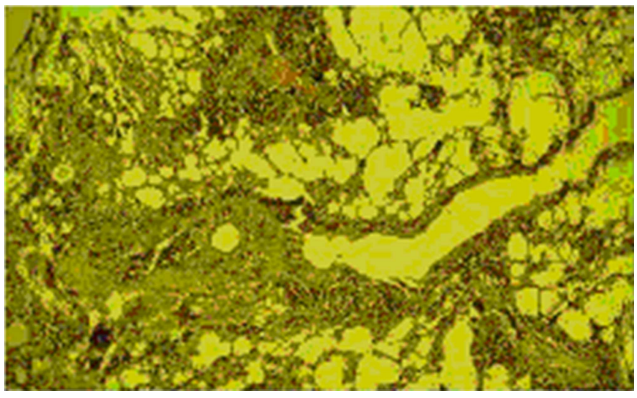

Figure 1. Original tissue image.

BACKGROUNDS

In the literature, several methods have been introduced to facilitate more accurate image processing in the medical field (e.g. [5-10]). Currently, in order to handle inaccuracy and vagueness in medical images, the application of fuzzy logic and relations has become very popular (e.g. [11-13]). Some of these fuzzy methods are as follows.

Castiello et al. [11] present a neuro-fuzzy approach for the classification of image pixels into three classes: contour, regular or texture points. Exploiting the processing capabilities of a neural network, fuzzy classification rules are derived by learning from data and are applied to classify pixels in grey-level images. To derive a proper set of training data, the spatial properties of image features and a multi-scaled representation of images are considered. Tizhoosh et al. [12] propose a hybrid neuro-fuzzy system, consisting of fuzzy techniques and neural nets, for knowledge-based enhancement of mega voltage images. The fuzzy enhancement includes different contrast adaptation techniques and soft filtering, respectively. A modified associative memory is trained using a priori knowledge for image restoration. In order to consider the subjective demands of physicians, an observer-dependent overall system for contrast adaptation is also proposed. Nauck and Kruse [13] present an algorithm based on a common multilayer perceptron structure whose weights are modeled by fuzzy sets, and the activation, output and propagation functions are adapted accordingly. Mitra and Pal [14] present an algorithm based on a modified Kohonen classifier [15], where the input is modified to accept linguistic representations of crisp input values, and the output provides fuzzy decisions in the form of membership values. Feleppa and Yaremko [16] present an algorithm based on a mountain clustering algorithm introduced by Yager and Filev [17] and refined by Chiu [18]. The determined cluster centers are used to initialize a neuro-fuzzy system that is trained by an Adaptive-Network-based Fuzzy Interference System (ANFIS), proposed by Jang [19]. Nozaki et al. [20] present a method based on the division of the pattern input space by equally spaced membership functions. This approach leads to a fuzzy set with a high number of rules.

Generally, image-processing methods have limitations when the image contains shadows and/or missing boundary segments and/or etc. An acceptable method for image processing should have less user interaction due to its drawbacks such as time consumption and human error, and it must be robust with respect to the presence of noise and shadows.

Based on the above reviews, in this paper, a new fuzzy method is proposed for segmentation and feature

extraction stages to improve the performance of the current algorithms.

THE PROPOSED APPROACH

In this section, we present new fuzzy methods for canny edge detection and Hough transform object extraction in digital image processing. The proposed approach contains five main stages (see Figure 2 and, for more details, see Figure 3):

- Pre-processing: After smoothing, using a Gaussian low pass filter, a primary version of the image with sufficient contrast is produced.
- Segmentation: The segmentation stage consists of three main steps: 1) Coarse segmentation of the RGB (Red, Green and Blue layers of a digital image) image by separating the three base colors of red, green and blue; 2) Using an edge based model segmentation, a novel fuzzy canny edge detection, for detecting edges in the image; 3) Using a fuzzy c-means clustering method as a pixel-based model for selective segmentation of different objects in our image.
- Feature Extraction: After segmentation, which highlights the main features in our image and works as a data reduction tool, extraction of the selected features, in order to be accessible for analyzing, is done by using a new fuzzy Hough transform, which detects vessels and bronchioles in our image.
- Approximate Reasoning: By defining a fuzzy inference system, based on the produced membership functions with fuzzy c-means clustering, which is a combination of Mamdani and Logical-modeling systems with a Yager parametric operator of combination for Mamdani and Logical inference and operators, analysis and diagnostics will be done.
- Learning and Tuning Parameters: In order to optimize the proposed system and tune the parameters such as the size of vessel/bronchiole radii, we used a feed forward neural network.

In the following subsections, each stage of the proposed approach will be explained in detail.

Pre-Processing

There are two main domains for image enhancement: 1) Enhancement in the spatial domain, where there are a different number of points in an image; 2) Enhancement in the frequency domain, where we consider an image as a collection of frequency components [21].

Figure 2. General schematic diagram of the proposed approach.

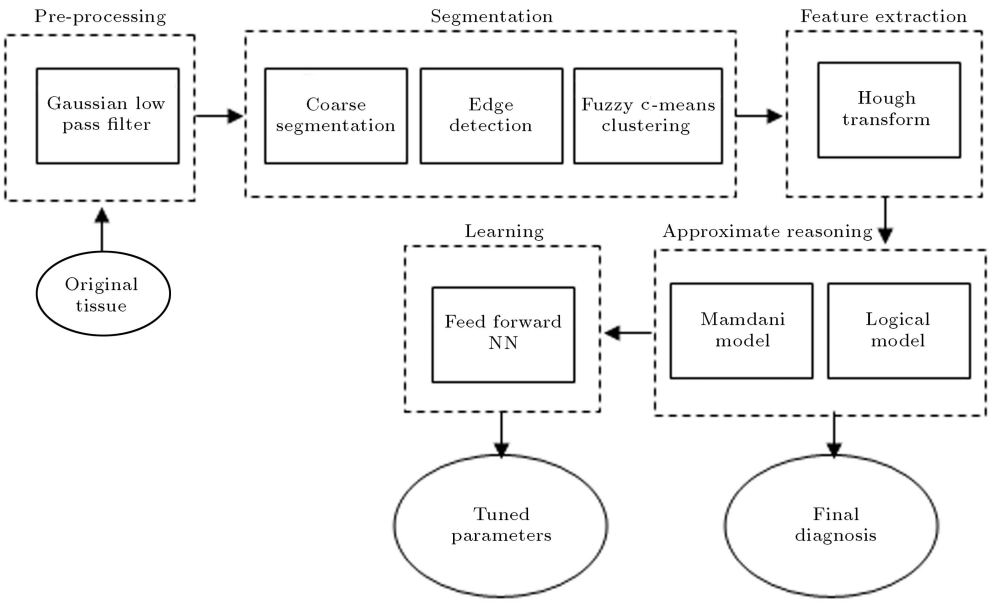

Figure 3. Detailed schematic diagram of the proposed approach.

There is a direct link between some of those spatial filters and their frequency domain counterparts. The most fundamental relationship between spatial and frequency domains is established by a well-known result called the convolution theorem [22]. The process, by which we move a mask from pixel to pixel in an image and compute a predefined quantity at each pixel, is the foundation of the convolution process. Formally, the discrete convolution of two functions, $f(x,y)$ and $h(x,y)$ of size $M \times N$, is denoted by $f(x,y)^* h(x,y)$ and is defined by the following expression:

$$f(x,y)^* h(x,y) = \frac{1}{MN} \sum_{m=0}^{M-1} \sum_{n=0}^{N-1} f(x,y) h(x-m, y-n). \quad (1)$$

Letting $F(u,v)$ and $H(u,v)$ denote the Fourier transforms of $f(x,y)$ and $h(x,y)$, respectively, one-half of the convolution theorem simply stated that $f(x,y)^* h(x,y)$ and $F(u,v)$ $H(u,v)$ constitute a Fourier transform pair. This result can formally be stated as:

$$f(x,y) * h(x,y) \Leftrightarrow F(u,v) H(u,v). \quad (2)$$

Filters in the spatial and frequency domains constitute a Fourier transform pair. Thus, given a filter in the frequency domain, the corresponding filter can be obtained in the spatial domain by taking the inverse Fourier transform of the former. The reverse is also true.

If both filters are of the same size, it is generally more efficient, computationally, to do the filtering in the frequency domain. Filtering is often more intuitive in the frequency domain. Generally, the narrower the frequency domain filter, the more the attenuated low frequencies resulting in increased blurring. In the spatial domain, this means a wider filter, which in turn implies a larger mask. The plots of these two functions for the Gaussian function are shown in Figure 4.

More complex filters can be constructed from the basic Gaussian functions [21]. For instance, we can construct a high pass filter as a difference of Gaussians, shown in Figure 5.

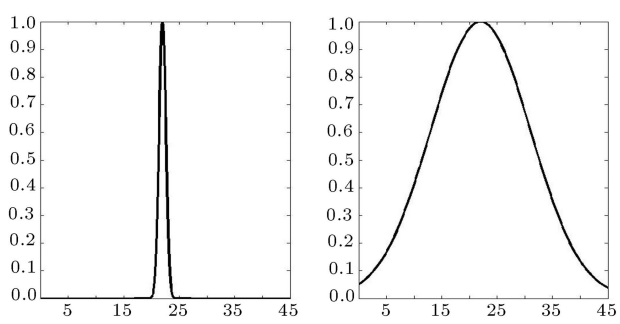

Figure 4. Gaussian frequency domain lowpass filter and Gaussian lowpass spatial filter.

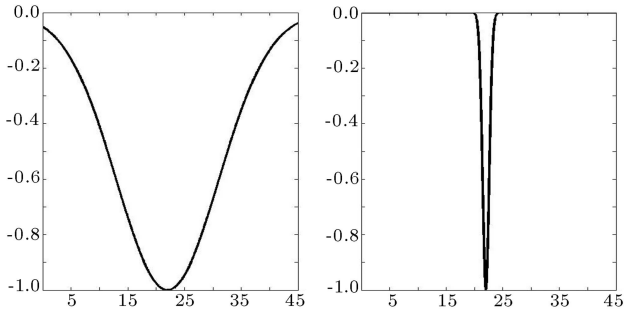

Figure 5. Gaussian frequency domain highpass filter and Gaussian highpass spatial filter.

In the frequency domain, we just have positive values without harmonies which makes it a little bit gross, but gives us an opportunity for faster (computer) processing [23,24].

In the preprocessing stage of the proposed program for tissue images, we use a Gaussian low pass filter, which is a smoothing filter in the frequency domain. The reason for choosing the frequency domain is the large size of the tissue images and related masks, where using the frequency domain facilitates computation and decreases time complexity (convolution in the spatial domain equals multiplication in the frequency domain).

Although the original image of the tissue is an RGB, we do not use this filter in the RGB domain. Before filtering, we segment the image based on three base color layers: Red, Green and Blue. According to the explanation in the next section, we chose blue images to be filtered, as in the Gaussian low pass filters (GLPFs) form, in two dimensions, which are given by [21]:

$$H(u,v) = e^{-D^2(u,v)/2\sigma^2}, \quad (3)$$

where $D(u,v)$ is the distance from the origin of the Fourier transform, which we assume has been shifted to the center of the frequency rectangle. By letting $\delta = D_0$ (in this program, we have chosen $D_0 = 2$), we can express the filter in a more familiar form in terms of the notation in this section:

$$H(u,v) = e^{-D^2(u,v)/2D_0^2}. \quad (4)$$

Segmentation

After enhancing the images and highlighting the chief features by segmenting the images, important objects will be more accessible and unnecessary objects will be removed, which is also a method for image compression. There are three stages of segmentation used in this study: 1) Coarse segmentation; separating RGB elements (Red, Green, Blue); 2) Fuzzy canny edge detection, which is the most powerful segmentation method in the edge based models; 3) The fuzzy c-means

clustering method, again a powerful tool in pixel-based models for segmentation.

In the first step of segmentation, we just separate the three basic elements of RGB images as demonstrated in Figure 6.

The canny edge detector, the most popular edge detection technique at present, is formulated with three main objectives [25]:

1. Optimal detection with no spurious responses;
2. Good localization with minimal distance between the detected and true edge position;
3. Single response to eliminate multiple responses to a single edge.

The first requirement is to reduce the response to noise. This can be affected by optimal smoothing, with Gaussian filtering, as mentioned before. The second criterion aims for accuracy: Edges are to be detected in the right place. This can be achieved by a process of non-maximum suppression (which is equivalent to peak detection). Non-maximum suppression retains only those points at the top of a ridge of edge data, while suppressing all others. This results in thinning: The output of non-maximum suppression is thin lines of edge points in the right place. The third constraint concerns the location of a single edge point in response to a change in brightness. This is because more than one edge can be denoted with the output obtained by earlier edge operators.

In order to mark an edge at the correct point and to reduce multiple responses, we can convolve an image with an operator, which gives the first derivative in a direction normal to the edge. The maximum of this function should be the peak of edge data, where the gradient in the original image is sharpest, and therefore the location is an edge. Accordingly, we seek an operator, G_n, which is a first derivative of a Gaussian function, g, in the direction of the normal, $n_\perp$:

$$G_n = \frac{\partial y}{\partial n_\perp}, \tag{5}$$

where $n_\perp$ can be estimated from the first-order difference of the Gaussian function, g, convolved with the image P and scaled, appropriately, as:

$$n_\perp = \frac{\nabla(P^* g)}{|\nabla(P^* g)|}. \tag{6}$$

The location of the true edge point is then at the maximum point of G_n convolved with the image. This maximum is when the differential along $n_\perp$ is zero:

$$\frac{\partial(G_n^* P)}{\partial n_\perp}, \tag{7}$$

$$\frac{\partial^2(G_n^* P)}{\partial n_\perp^2} = 0. \tag{8}$$

This is non-maximum suppression which is equivalent to retaining peak differentiation perpendicular to the edge, thinning the response of the edge detection operator to give edge points, which are in the right place without multiple responses and with a minimal response to noise.

Non-maximum suppression essentially locates the highest points in the edge magnitude data. This is performed by using edge direction information to check that points are at the peak of a ridge.

In order not to be misled by the local maximum of the non-maximum suppression algorithm, we use a Hysteresis filter, which sets the points to white once they are above the upper threshold and sets them to black when they are under the lower threshold and the grade in between two thresholds can be defined; here, we choose them equal to one. The power of the canny edge detector lies in these two algorithms, but one of the most important things is choosing the best threshold for the real edge, where a threshold set to high can miss important information, while a threshold set to low will falsely identify irrelevant information as important. It is difficult to give a generic threshold that works well on all images. No tried and tested approach to this problem yet exists. In this study, we propose an algorithm for determining the thresholds as follows.

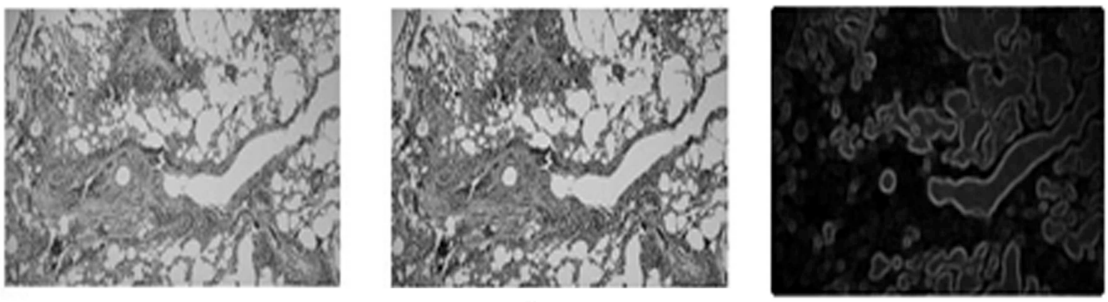

Red image Green image Blue image

Figure 6. Coarse segmentation of RGB image.

Threshold Algorithm

As mentioned before, the use of a threshold is for omitting the local maxima and decreasing the noise effect in a non-maximum suppression algorithm. The steps of the proposed algorithm are as follows:

Step 1- Choose the blue segment of the original image for edge detection because of its sharp edges and less noise.

Step 2- Change the type of image from RGB to an intensity image, where the edges are shown by higher intensity.

Step 3- Change the intensity image to a magnitude image (computed gradients) through a non-maximum suppression algorithm. By this time, we have the gradient value of each pixel as shown in Figure 7.

Step 4- Use a fuzzy c-means algorithm to define 3 clusters in the magnitude image, which are: 1) Zero defined; 2) Local maxima and 3) The maximum gradients.

Step 5- Define the points with maximum intensity values (gradients); the points in the 3rd cluster as the edges.

The application of non-maximum suppression and the fuzzy c-means threshold is demonstrated in Figure 8.

The action of non-maximum suppression is to select the point along the top of the ridge. Given that the top of the ridge initially exceeds the upper threshold, the threshold output is then set to black until the peak of the ridge exceeds the upper switching threshold. The result of the proposed fuzzy canny edge detection is shown in Figure 9.

RGB images are a combination of three base colors of red, green and blue and the color of objects that we see is based on the rate of combination of these three. If the rate of red is greater than the other two colors, the object seems to be red and so on. Therefore, for basic extraction of features in the images, we use a fuzzy clustering method, fuzzy c-means [3,26], for partitioning each color layer separately. The number of clusters would be the number of objects in the image (epithelial layer, tissue, background). By this method, during the process of our algorithm, we just focus on the essential parts of the image and leave the other parts. This, again, helps to reduce data and decrease computation complexity, while working precisely on the essential parts. A sample of the tissue image, with its related membership functions, used for extracting objects is shown in Figure 10.

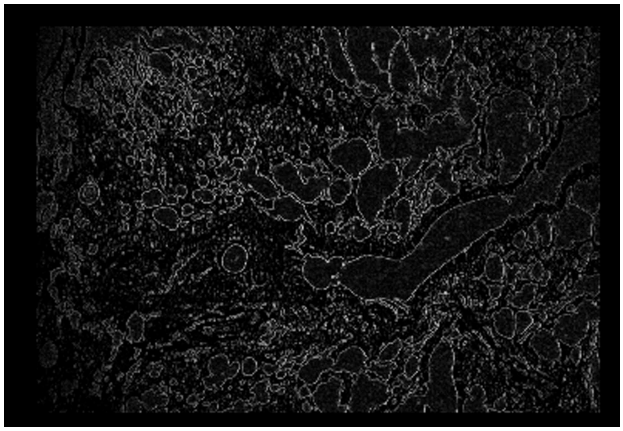

Figure 7. The magnitude image.

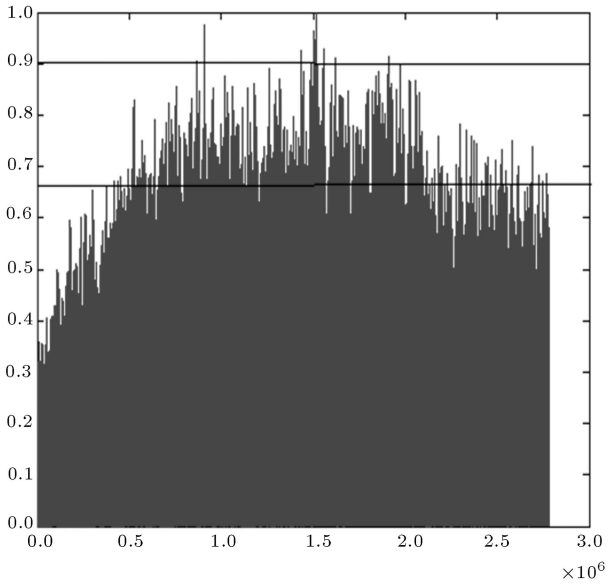

Figure 8. Non-maximum suppression and fuzzy c-means threshold.

Figure 9. The result of fuzzy canny edge detector.

Feature Extraction

High-level feature extraction concerns finding shapes in computer images. Shape extraction implies finding

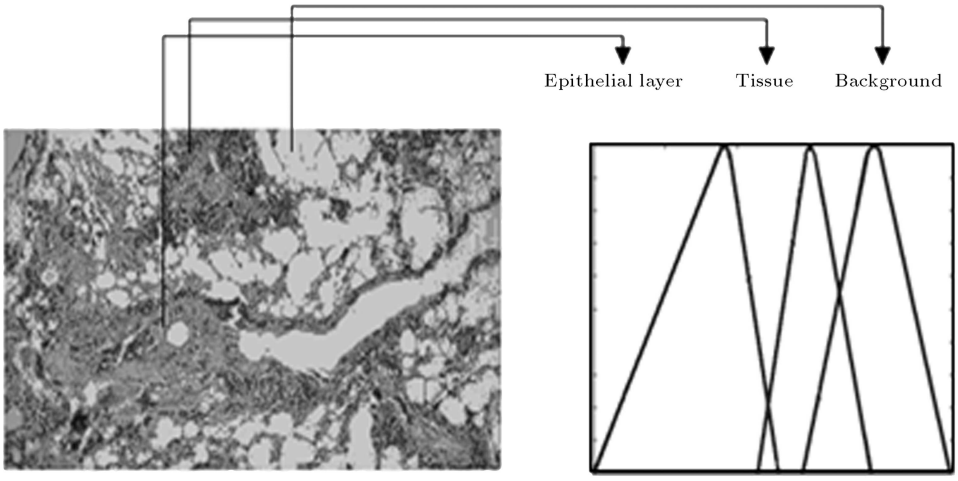

Figure 10. Original tissue image with its related membership function used for extracting objects during segmentation stage.

their position, orientation and size [25]. In order to diagnose inflammation in the tissue images, thick cell layers around the vessels and bronchus must be detected. The shape of the section of vessels and bronchus is approximately a circle and, for that reason, we choose a new fuzzy Hough Transform (HT) for extracting these sections and checking around them for diagnosing inflammation.

In an explicit form of the equation, the HT can be defined by considering the equation for a circle, given by:

$$(x - x_0)^2 + (y - y_0)^2 = r^2. \tag{9}$$

This equation defines a locus of points (x, y) centered on an origin (x_0, y_0) within which, in this program, we search for the centers of every pixel with a distance equal to 2 pixels from the previous one and with radius r, which is defined according to the magnification of the microscope for imaging. After gathering evidence of all the edge points, the maximum in the accumulator space again corresponds to the parameters of the circle in the original image. The center of an image in an accumulator space is distinguished by the maximum value. But, in complicated images such as tissue images, there is usually more than one circle, and thus the related centers are more than one. This means that choosing the maximum is not adequate for such images. Therefore, in this study, we propose an algorithm to choose maximum ranges instead of choosing a single maximum.

Thresholding Algorithm for Accumulator Space

By clustering the accumulator space into three parts of ordinary points, noise and centers, we could easily access the center cluster and define our threshold. However, as the majority of pixels in an image are not centers, clustering the whole image would result in determining clusters with low value centers. To avoid such a problem, the following algorithm is presented:

Step 1- Omit the points that have a value of less than 0.5 in the normalized accumulator space before clustering, because the focus is on the high values of the accumulator for determining the maximum range.

Step 2- Cluster the remaining data into two parts of centers and noise.

Step 3- Choose the minimum value of the first cluster for defining the threshold, as demonstrated in Figure 11.

After thresholding and defining centers, according to the defined radius, the circles, as a symbol of vessels and bronchus, would be extracted, as shown in Figure 12.

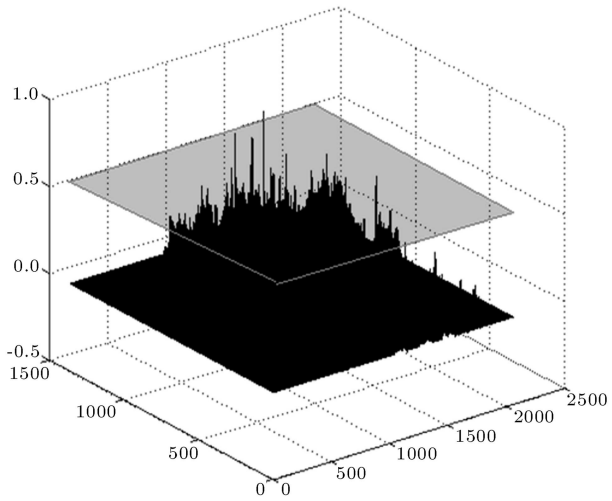

Figure 11. Thresholding the accumulator space for defining maximum ranges.

Figure 12. Extracting circle by Hough transform.

Moreover, in order to check the precision of the proposed algorithm, the extracted circles are marked in the original image, as illustrated in Figure 13.

Approximate Reasoning

After detection and extraction of the needed object, the next step is to analyze the image according to the evidence for diagnosis. Here, we deal with a fuzzy qualitative model and reasoning method (as a system model) based on linguistic descriptions, just as we use them in the process of medical diagnosis.

We go beyond this stage by utilization of the concept of linguistic approximation. This is given a conventional fuzzy model with fuzzy sets. We improve its qualitative nature by using linguistic approximation techniques in fuzzy logic.

The identification of a fuzzy model is divided into two parts [27]: 1) Structure identification; and 2) Parameter identification. Structure identification of a system has to solve two problems: finding input variables and the input-output relation. In this study,

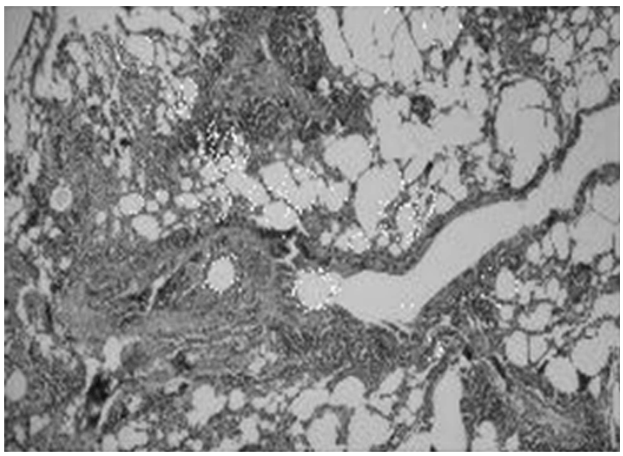

Figure 13. Fitting the extracted circles on the original image.

as the medical specialist defined, there are 4 ranges of inflammation. The degree of inflammation is defined according to the smoothness and reshaping of the epithelium layer around the vessels and bronchus and the thickness of their wall. Therefore, the number of rules for diagnosing inflammation must be four, where each rule defines one of the grades of inflammation in the image. In the antecedent, we would have a sign of smoothness and thickness and in consequence the defined grade of inflammation.

The thickness of the cell layer and smoothness around the vessels and bronchioles is defined by the red pixels in the red layer of the image, which are in the cluster of epithelial layers defined by fuzzy c-means clustering in the segmentation stage. Diagnosing thick cell layers is based on counting the cell layer around the object. In this study, the number of cell layers around the object is approximated by a distance measure. The proposed method is as follows:

Step 1- Define different neighborhood windows whose size is from r up to $r+4L$, where r is the radius of the feature and L is the estimated thickness of one cell layer.

Step 2- Compute the average value of the red pixels in the epithelial layer cluster in each of the neighborhood windows, as an approximation for the thickness of layers around the object.

Clustering the computed averages in four ranges, we would have the measure of sensing thick cell layers; assuming that the first cluster illustrates the 1st cell layer and the second cluster illustrates the 2nd cell layer and so on. A sample of defined clusters is shown in Figure 14.

Up to this stage, we have an estimation of the number of epithelial cells that make the premises. The output of the system is a diagnosis degree of inflammation from 1 to 4, but as the cell layers around the objects are not precisely arranged, we could not cluster this four degree of inflammation crisply. They have some overlaps between their clusters. For this reason, we use a fuzzy c-means for clustering the neighborhood around the vessel/bronchus section in four levels according to distance. A sample of the defined clusters is illustrated in Figure 15.

In the parameter identification stage, we determine the parameter of fuzzy membership functions. In this paper, we approximate the convex fuzzy set with a Gaussian fuzzy set by defining the mean and sigma, as shown in Figure 16. In this image, the dashed line is the membership function and the continuous line is estimation with a Gaussian function.

In other words, we define the following rules, as illustrated in Figure 17:

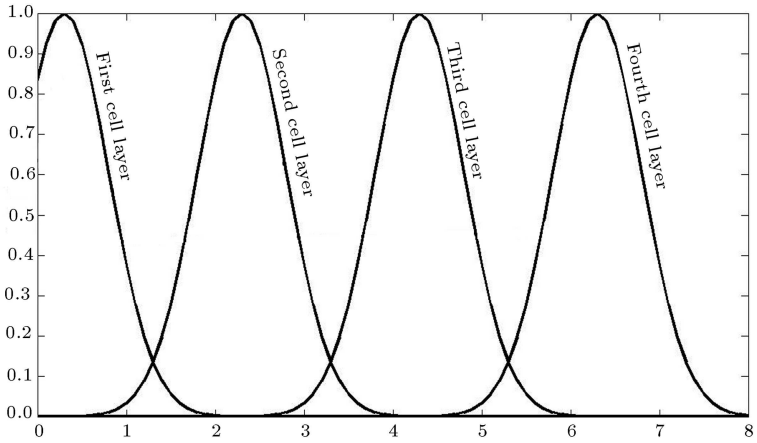

Figure 14. Input cluster (estimation of number of cell layers).

1. If the average red in the first cluster is small, then it is inflammation degree 1;
2. If the average red in the second cluster is low medium, then it is inflammation degree 2;
3. If the average red in the third cluster is high medium, then it is inflammation degree 3;
4. If the average red in the fourth cluster is large, then it is inflammation degree 4.

The method of inference is a combination of Mamdani and Logical modeling systems with a Yager parametric operator of combination for Mamdani and Logical and other operators. Given a decreasing generator, f, the Yager intersection and union (t-norm and s-norm) are defined as follows [2]:

t-norm,:

$$f_w(a) = (1-a)^w \qquad (w > 0), \tag{10}$$

$$f_w^{(-1)}(z) = \begin{cases} 1 - z^{1/w} & \text{when } z \in [0,1] \\ 0 & \text{when } z \in (1,\infty) \end{cases} \tag{11}$$

$$i_w(a,b) = f_w^{(-1)}((1-a)^w + (1-b)^w)$$
$$= 1 - \min(1, [(1-a)^w + (1-b)^w]^{1/w}), \tag{12}$$

s-norm:

$$g_w(a) = a^w \qquad (w > 0), \tag{13}$$

$$g_w^{(-1)}(z) = \begin{cases} z^{1/w} & \text{when } z \in [0,1] \\ 1 & \text{when } z \in (1,\infty) \end{cases} \tag{14}$$

$$u_w(a,b) = g_w^{(-1)}(a^w + b^w) = \min(1, (a^w + b^w)^{1/w}). \tag{15}$$

In the linguistic fuzzy models, Logical and Mamdani models (both the antecedent and the consequent) are fuzzy propositions. The general forms of linguistic fuzzy if-then rules for Mamdani and Logical are [28,29]:

Mamdani model:

$$R_i: \text{ if } x \text{ is } A_i, \text{ then } y \text{ is } B_i, \quad i = 1, 2, \cdots, K.$$

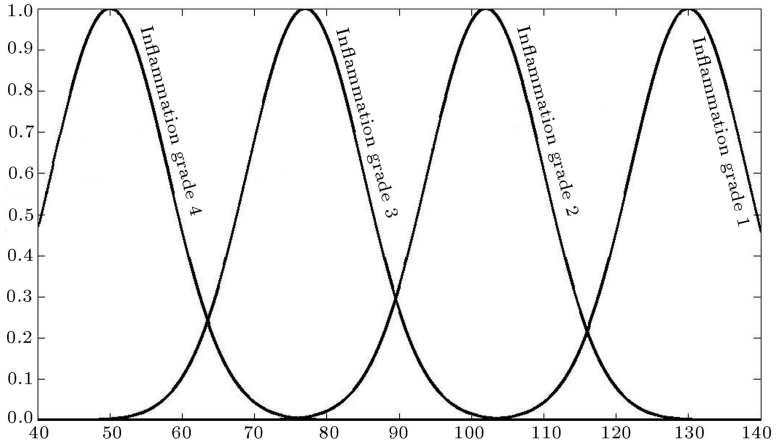

Figure 15. Output cluster (estimation of inflammation).

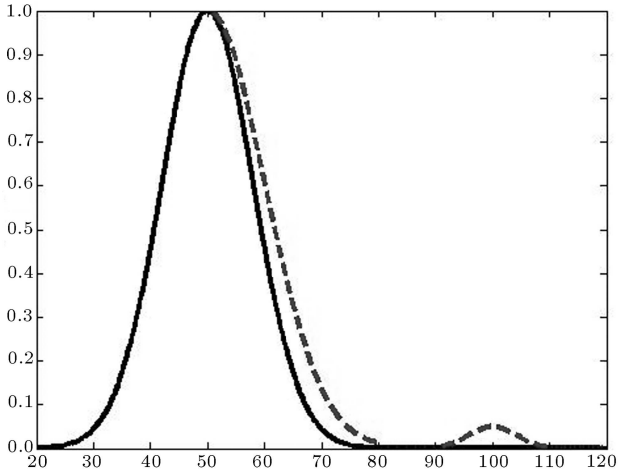

Figure 16. Gaussian fuzzy set.

Logical model:

$$R_i: \text{ if } x \text{ is } \bar{A}_i, \text{ then } y \text{ is } B_i, \quad i = 1, 2, \cdots, K \ ,$$

where x is the antecedent variable, y is the consequent variable, A_i and B_i are linguistic terms (fuzzy sets) defined by multivariate membership functions, respectively, and K denotes the number of rules in the model. The Mamdani and Logical Inference models are shown in Figures 18 and 19.

The Yager unified fuzzy reasoning method for combination of the Mamdani and Logical model is defined as follows [26]:

$$\mu_E(y) = \beta\mu_{\text{Logical}}(y) + (1-\beta)\mu_{\text{Mamdani}}(y), \qquad (16)$$

where μ is the result of each method and β is defined from 0 (Mamdani), to 1 (Logical).

The defuzzification method is the center of area method [26,30], which is also called the center of gravity method. The crisp value is simply the centroid or the resultant membership function:

$$d_{CA}(A) = \left(\int A(z)z\,dz\right) / \left(\int A(z)dz\right). \qquad (17)$$

This is the most common method used and every part of the membership function contributes to the final answer.

LEARNING AND TUNING PARAMETERS

Tuning the parameters, such as the size of the radius for feature extraction with the Hough transform, is done by a feed-forward neural network through supervised learning with back error propagation. Given a set of input-output pairs, it is highly desirable to be able to

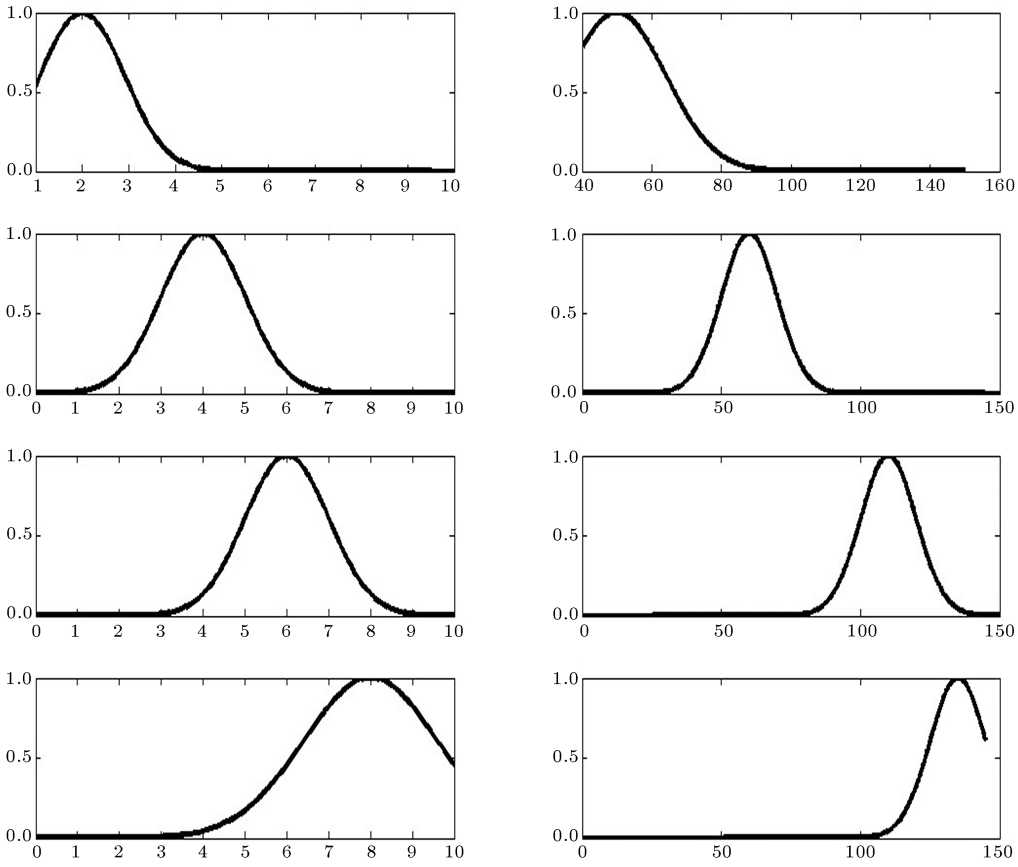

Figure 17. Proposed rule base.

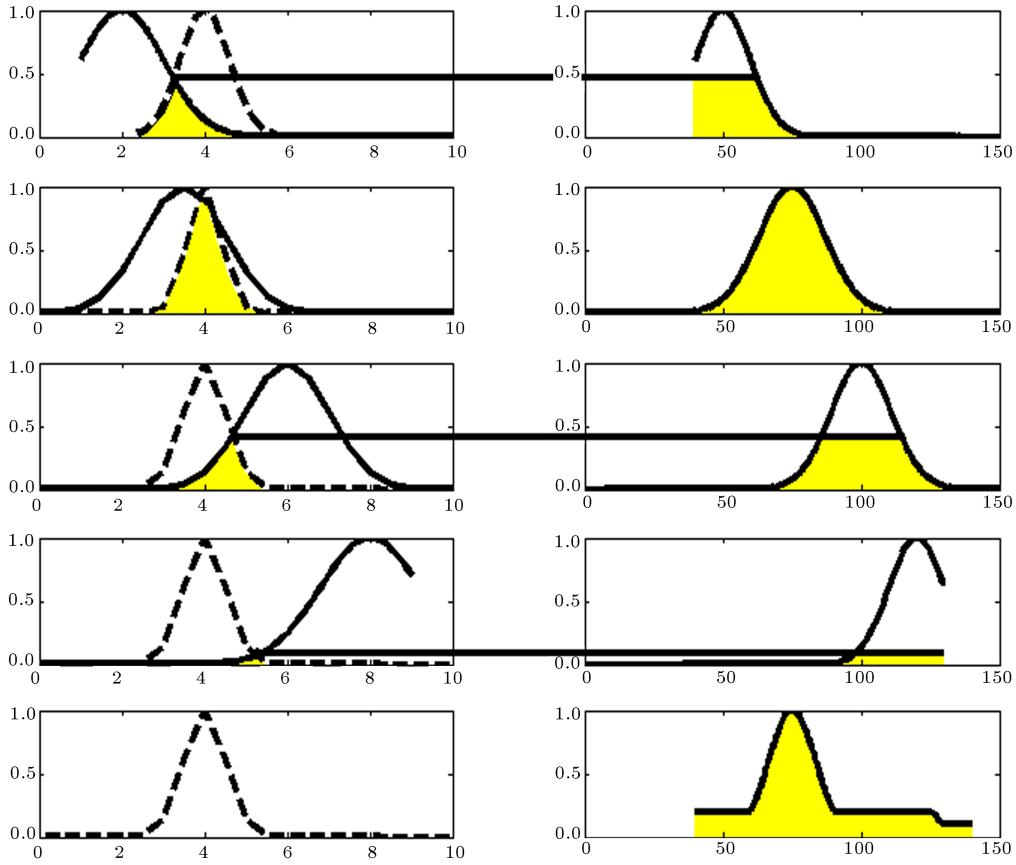

Figure 18. Mamdani inference model.

determine the weights directly from the given data. This problem has been solved using the generalized data rule. The use of this rule has greatly enhanced the usage of neural networks. The basic idea of training a feed forward neural network is to generalize the delta rule for each weight. Given a set of input-output pairs, $< X, D >$, and a neural network, the problem at hand is to find the weights of the neurodes for the layer. The output of the jth neurode in the output layer is obtained from the associated inputs to that neurode [22,31]:

$$O_j^o = f(Wx). \tag{18}$$

The superscript "o" denotes the output layer. Cost function can be defined as squared output error:

$$E = \sum (d - O_j^o)^2. \tag{19}$$

The weights to the jth neurode can immediately be determined by finding the gradient of the squared error, according to the weight of interest, denoted as:

$$\nabla w_{ij}(E). \tag{20}$$

The weight update equation is derived from the negative gradient and can be written as follows:

$$\Delta w_{ij}^o = -\eta \nabla w_{ij}(E), \tag{21}$$

where $\eta > 0$ is the step size or learning constant and is a small positive constant. If the "error" of the output neurodes is defined as:

$$\delta_{oj} = (d_K - O_j^o) O_j^o f'(Wx). \tag{22}$$

The way update equations for the output layer can be written as:

$$\Delta w_i = \eta \delta_{oj} y_i, \tag{23}$$

then, the update equation is obtained by repeatedly applying the chain rule to the cost function.

Learning Rate and Momentum

The convergence rate of the update process is governed by step size η, sometimes known as the learning constant. If η is small, then convergence is slow because the weights are updated by small increments. On the other hand, if η is large, then convergence is rapid because each update to weight moves the weight a significant amount. However, if η is too large, then an overshoot of the parameter values often occurs, causing oscillatory behavior. This leads to slow convergence again. In some cases, overshoots may also diverge the proper setting of the learning constant, which is very crucial. In this research, we use the following terms for tuning: $\eta = 0.05$; $E = 0.08$.

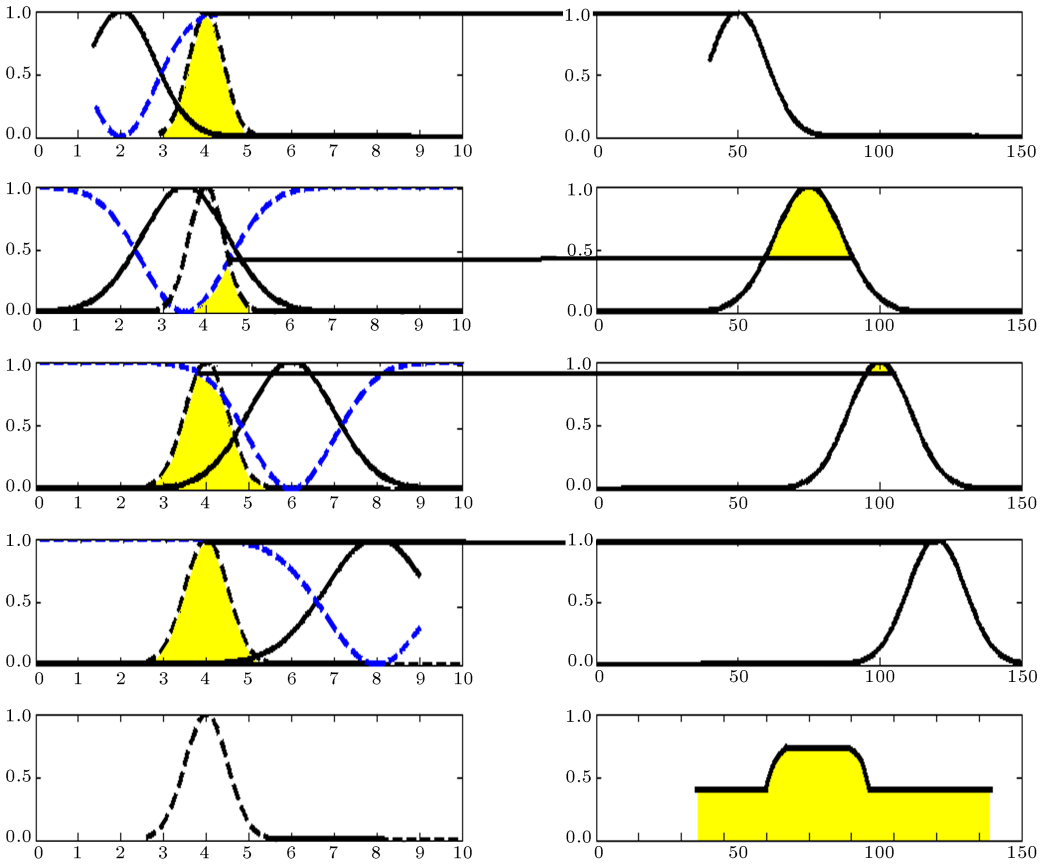

Figure 19. Logical inference model.

EXPERIMENTAL RESULTS

The proposed fuzzy approach to edge detection and feature extraction has improved the results in some way. We have selected the image to include regular and difficult cases and examined 10 different images. Actually, we have extracted many images for this research (almost 200). However, the selected images are the ones which include lots of uncertainties. The images were noisy with low contrasts. The selected images are the ones that include many uncertainties, being samples of the four grades of inflammation and could be considered as representations of each inflammation grade.

The results of the proposed method have been evaluated by comparing the proposed algorithm with the existing one. As mentioned throughout the paper, some parameters such as the size of the radius for feature extraction with the Hough transform, need to be adjusted in this algorithm. But, for a set of similar images, most of them do not require any change. In the experiment, the following configuration has been used:

- The radius of the circle for feature extraction with the Hough transform is [50 55]. For quantitative evaluation compared to the conventional ones for the same images, we have used a back propagation error measure to validate the performance of our algorithm for feature extraction. The results are shown in Table 1.

As shown, the performance of the proposed feature extraction method has been improved. This improvement could improve medical diagnoses and provide better results, because feature extraction is an important step in image processing. This is because powerful approximate reasoning is essential for having an accurate diagnostic system and the extracted features in this step are inputs of the approximate reasoning step.

Moreover, using fuzzy canny edge detection, compared with original canny edge detection, has the following results, as shown in Table 2.

Considering the quality of the images, the quantitative results are promising.

Table 1. Quantitative evaluation of proposed approach in comparison with conventional form.

	E (error)	**Performance**
Hough transform	0.1	0.9
Fuzzy Hough transform	0.08	0.92

Table 2. Quantitative evaluation of proposed approach in comparison with conventional form.

	No. Edge Points	Time of Computation
Canny edge detector	61011	23 min
Fuzzy canny edge detector	14114	5 min

CONCLUSION AND FUTURE WORKS

In this paper, a novel fuzzy modeling approach for edge detection and feature extraction has been presented. We first smoothed the original image using a Gaussian filter. This smoothed image is segmented, using a three level process composed of coarse segmentation (distributing the RGB), fuzzy canny edge detection and a fuzzy c-means clustering algorithm. The output image is ready for extracting highlighted features in the previous stages. Then, by using a fuzzy Hough transform for extracting circles, the focus is more transparent. For approximate reasoning, a fuzzy inference system with a combination of the Mamdani and Logical models is implemented. Finally, the parameters of the generated fuzzy model are tuned by using neural networks. In this approach, we have designed a straightforward and fast algorithm with rational level of user interaction. Using the proposed approach, the physicians can overcome the main problems of image processing which need expensive computation and are based on experimental adoptions.

In future research, we are going to develop a fuzzy adaptive approach for this purpose. Using a fuzzy adaptive approach for image enhancement and noise reduction, the image quality, especially the image edges, could be improved. That can give us better results in subsequent stages of diagnoses.

REFERENCES

1. Ellis, R., Leigh, R., Southam, D., O'Byrne, P.M. and D.Inam, M. "Morphometric analysis of mouse airways after chronic allergen challenge", *United States and Canadian Academy of Pathology*, **83**(9), pp. 1285-92 (2003).
2. Henderson, W.R.J., Tang, L., Chu, S.J., Tsao, S.M., Chiang, G.K., Jones, F., Jonas, M., Pae, C., Wang, H. and Chi, E. "A role for cysteinyl leukotrienes in airway remodeling in a mouse asthma model", *Am. J. Respir. Crit. Care Med.*, **165**, pp. 108-118 (2002).
3. Ebrina, M., Takahashi, T. and Chiba, T. "Cellular hypertrophy and hyperplasia of airway smooth muscles underlying bronchial asthma: A 3-D morphometric study", *Am. Rev. Respir. Dis.*, **148**, pp. 720-726 (1993).
4. Temelkovaski, J., Hogan, S.P., Shepherd, D.P., Foster, P.S. and Kumar, R.K. "An improved murine model of asthma: Selective airway inflammation", *Epithelial Lesions and Methacholine Responsiveness Following Chronic Exposure to Aerosolised Allergen*, **53**, Thorax, pp. 849-856 (October 1998).
5. Sahba, F., Tizhoosh, H.R. and Salama, M.M. "A course-to-fine approach to prostate boundary segmentation in ultrasound images", *Biomedical Engineering Online*, **4**, pp. 58-71 (October 2005).
6. Egmont-Petersen, M., de Ridder, D. and Handels, H. "Image processing with neural networks- A review", *Pattern Recognition*, **35**, pp. 2279-2301 (2002).
7. Betrounia, N., Vermandela, M., Pasquierc, D., Maucheb, S. and Rousseaua, J. "Segmentation of abdominal ultrasound images of the prostate using a priori information and adapted noise filter", *Computerized Medical Imaging and Graphics*, **29**, pp. 43-51 (2005).
8. Soltanian-Zadeh, H., Rafiee-Rad, F. and Pourabdollah-Nejad, D.S. "Comparison of multiwavelet, wavelet, haralic and shape feature for microcalssification classification in mammograms", *Pattern Recognition Society*, **37**, pp. 1973-1988 (April 2004).
9. Abdolmaesumi, P. and Sirouspour, M.R. "Segmentation of prostate contours from ultrasound images", *ICASSP04*, **3**, pp. 517-520 (2004).
10. Hassanien, A. "Fuzzy rough sets hybrid scheme for breast cancer detection", *Image and Vision Computing*, **25**, pp. 172-183 (2007).
11. Castillo, C., Castellano, G., Caponetti, L. and Fanelli, A.M. "Fuzzy classification of image pixels", Department of Information, Bari Univercity, Italy (2001).
12. Tizhoosh, H.R., Krell, G. and Michaelis, B. "Knowledge-based enhancement of megavoltage images in radiation therapy using a hybrid neuro-fuzzy system", *Image and Vision Computing*, **19**, pp. 217-233 (July 2000).
13. Nauk, D. and Kruse, R. "NEFCLASS-A neuro fuzzy approach for the classification of data", *Symposium on Applied Computing*, Nashville, USA (1995).
14. Mitra, S. and Pal, K. "Self-organizing neural network as a fuzzy classifier", *IEEE Transaction on Systems, Man, and Cybernetics*, **24**(3), pp. 385-399 (1994).
15. Kohonen, T., *Self-Organizing Maps*, 2nd Ed., New York, Springer Verlag (1997).
16. Feleppa, E.J. and Yaremko, M.M. "Ultrasonic tissue characterization for diagnosing and monitoring", *IEEE Eng. Med. Biol. Mag.*, **6**(4), pp. 18-26 (Dec. 1987).
17. Yager, R. and Filev, D. "Generation of fuzzy rules by mountain-clustering", *Journal of Intelligent and Fuzzy Systems*, **2**(3), pp. 209-219 (1994).
18. Chiu, L. "Fuzzy model identification based on cluster estimation", *Journal of Intelligent and Fuzzy Systems*, **2**, John Wiley and Sons, pp. 267-278 (1994).
19. Jang, R. "ANFIS: Adaptive-Network-Based-Fuzzy-Inference-Systems", *IEEE Transactions on Systems, Man, and Cybernetics*, **23**(3), pp. 665-685 (1993).

20. Nozaki, K., Ishibushi, H. and Tanaka, H. "Trainable fuzzy classification system based on fuzzy If-then rules", *Proc. IEEE*, **1**, pp. 498-502 (1994).
21. Gonzalez, R.C. and Wood, R.E., *Digital Image Processing*, Prentice Hall (2002).
22. Hlawitschka, M., Ebling, J. and Scheuermann, G. "Convolution and fourier transform of second order tensor fields", *Proceedings of Visualization, Imaging and Image Processing Conference*, Marbella, Spain, pp. 452-458 (Sep. 6-8 2004).
23. Oppenheim, A.V. and Willsky A.S., *Signals and Systems*, Prentice Hall (1997).
24. Oppenheim, A.V., *Advanced Topics in Signal Processing*, Engelwood Cliffs, Prentice Hall (1998).
25. Nixon, M. and Aguado, A. "Feature extraction and image processing", *Newnes* (2002).
26. Klir, G.J. and Yuan, B., *Fuzzy Sets and Fuzzy Logic Theory and Application*, Prentice Hall of India, New Dehli (2002).
27. Sugeno, M. and Yasukawa, T. "A fuzzy-logic-based approach to quantitative modeling", *IEEE Transactions on Fuzzy Systems*, **1**(1), pp. 7-31 (February 1993).
28. Babuska, R., *Fuzzy Modeling for Control*, Kluwer Academic Publishers Boston / Dordrecht / London (1998).
29. Dvorak, A. "Properties of the generalized fuzzy logical inference", *Proc. Int. Panel Conf. on Soft and Intelligent Computing*, Technical Univ. of Budapest, Budapest, pp. 75-80 (1996).
30. Lee, C.C. "Fuzzy logic in control systems: Fuzzy logic controller", *IEEE Transactions Systems, Man and Cybernetics*, **II**, pp. 404-418 (1990).
31. Nagaraja, G. and Bose, R.P.J.Ch. "Adaptive conjugate gradient algorithm for perceptron training", *Neurocomputing*, **69**, pp. 368-386 (January 2006).